European Journal of Medicinal Chemistry 184 (2019) 111751

Contents lists available at ScienceDirect

European Journal of Medicinal Chemistry

journal homepage: http://www.elsevier.com/locate/ejmech

Research paper

Strong *in vitro* and *vivo* cytotoxicity of novel organoplatinum(II) complexes with quinoline-coumarin derivatives

Qi-Pin Qin [a, b, *], Zhen-Feng Wang [a], Xiao-Ling Huang [a], Ming-Xiong Tan [a, **], Bi-Qun Zou [b, c, d, ****], Hong Liang [b, ***]

[a] Guangxi Key Lab of Agricultural Resources Chemistry and Biotechnology, College of Chemistry and Food Science, Yulin Normal University, 1303 Jiaoyudong Road, Yulin, 537000, PR China
[b] State Key Laboratory for the Chemistry and Molecular Engineering of Medicinal Resources, School of Chemistry and Pharmacy, Guangxi Normal University, 15 Yucai Road, Guilin, 541004, PR China
[c] Department of Chemistry, Guilin Normal College, 9 Feihu Road, Gulin, 541001, China
[d] School of Pharmacy, Guilin Medical University, Guilin, 541004, China

ARTICLE INFO

Article history:
Received 24 July 2019
Received in revised form
29 September 2019
Accepted 30 September 2019
Available online 2 October 2019

Keywords:
quinoline-coumarin derivatives
Organoplatinum(II) complexes
Cell apoptosis
Mitochondria dysfunction

ABSTRACT

A series of novel organoplatinum(II) complexes, [Pt^{II}(QC1)(H-QC1)Cl] (**Pt1**), [Pt^{II}(QC2)(H-QC2)Cl] (**Pt2**), [Pt^{II}(QC3)(H-QC3)Cl] (**Pt3**), [Pt^{II}(QC4)(H-QC4)Cl]·CH_3OH (**Pt4**), [Pt^{II}(QC5)(H-QC5)Cl] (**Pt5**), [Pt^{II}(H-QC6)$(DMSO)Cl_2$] (**Pt6**), [Pt^{II}(H-QC7)$(DMSO)Cl_2$]·H_2O (**Pt7**), [Pt^{II}(H-QC8)$(DMSO)Cl_2$] (**Pt8**), [Pt^{II}(H-QC9)$(DMSO)Cl_2$]·CH_3OH (**Pt9**), [Pt^{II}(H-QC10)$(DMSO)Cl_2$] (**Pt10**) and [Pt^{II}(H-QC11)$(DMSO)Cl_2$] (**Pt11**), bearing quinoline-coumarin derivatives (H-QC1−H-QC11) have been first designed. Complexes **Pt1**−**Pt11** selectively displayed obvious cytotoxicities in comparison to cisplatin for A549/DDP (cisplatin-resistant human lung adenocarcinoma) cells and HeLa cervical carcinoma cells, with IC_{50} values as low as 100 nM−10.33 μM. In addition, **Pt4** and **Pt5** display a green-colored luminescent properties, targeted mitochondrial membrane and, thereby induced mainly mitochondria-mediated cell apoptosis was in the following order: **Pt4** > **Pt5**. The different anti-cancer activity of quinoline-coumarin complexes **Pt4** (100 nM) and **Pt5** (250 nM) were correlate with the presence of 3-(2′-quinolyl)-6-hydroxy-coumarin (H-QC4) ligand. The quinoline-coumarin complex **Pt4** (2.0 mg/kg per 2 days) also displayed potent *in vivo* anti-tumor effect after 21 days-treated. In contrast, the H-QC4 ligand highly enhances the anti-tumor activity and selectivity of organoplatinum(II) complexes in comparison to other previously reported coumarin derivatives metal complexes.

1. Introduction

Pt-based anti-tumor drugs, such as cisplatin and its ramification, have become important complexes in many tumor types therapy [1–7]. Unfortunately, the highly side effects (high toxicity) and drug-tolerance of Pt-based drugs and, thereby limiting their clinical therapy [8–20]. To overcome these shortcomings of cisplatin and its antiproliferative derivatives, different methods have been explored [21–24], including the study of organoplatinum(II) complexes, such as iminophosphorane cyclometalated-Pt(II) complexes [21], oxoisoaporphine Pt^{II} complexes [25], 3-(2′-benzimidazolyl)-7-methoxycoumarin Pt^{II} complex [26], rhomboidal Pt^{II} metallacycles [27], C,N-dimethylbenzylamine cycloplatinated Pt^{II} compounds [28], nucleobases and their derivatives organoplatinum(II) complexes [29], 1,5-cyclooctadiene and alkynyl Pt^{II} complexes [30,31], luminescent cyclometalated Pt^{II} complex [32], N,N-dimethyl-1-(2-aryl)methanamine-κ_2C_2,N organometallic Pt^{II} complexes [33], and curcumin organoplatinum(II) metallacycle [34], *etc.*

Since coumarin and its metal complexes possesses anti-cancer, anti-HIV, anti-Alzheimer effects, and most of them have been extensively considered as an ideal anti-tumor agents and a telomerase inhibitor [35–46]. For example, Özdemir reported that

* Corresponding authors. Guangxi Key Lab of Agricultural Resources Chemistry and Biotechnology, College of Chemistry and Food Science, Yulin Normal University, 1303 Jiaoyudong Road, Yulin, 537000, PR China
** Corresponding author.
*** Corresponding authors.
**** Corresponding author. Department of Chemistry, Guilin Normal College, 9 Feihu Road, Gulin, 541001, China
E-mail addresses: qpqin2018@126.com (Q.-P. Qin), mxtan2018@126.com (M.-X. Tan), zoubiqun@163.com (B.-Q. Zou), hliang@mailbox.gxnu.edu.cn (H. Liang).

https://doi.org/10.1016/j.ejmech.2019.111751
0223-5234/

coumarin-thiazole Pd^{II} complex has the most anti-cancer activity against LNCaP cells, with IC_{50} value was 10.05 μg/mL [45]. Kostova investigated the coumarins Ce(III) complex, which exhibited high cytotoxic against HL-60 cells (12.5−50.0 μM) by affecting programmed cell death [46]. Besides, a new coumarin derivative to monitor Cu(II) in cultured cells [42]. Paul and Bodio suggested that coumarin-phosphine Au^{III} complexes may induce cell death/apoptosis by interaction with related-protein(s) contained in lipid rafts [41]. In addition, Qin reported Pt^{II} and Ru^{II} complexes with 3-(2′-benzimidazolyl) coumarins as a telomerase inhibitor and c-myc G-quadruplex (G4) ligands [26,35,36]. On the basis of our first reported 3-(2′-benzimidazolyl) coumarins Pt(II) and Ru(II) complexes as potential anticancer agents [26,35,36], in order to exploit new Pt^{II} complexes with more extended planar coumarins derivatives ligands, herein, we first synthesized 11 new quinoline-coumarin derivatives (H-QC1−H-QC11) and their novel organoplatinum(II) complexes **Pt1**−**Pt11**. And the study of their anticancer (antiproliferative) effect against A549/DDP (cisplatin-resistant human lung adenocarcinoma) cells or HeLa cancer cells in comparison to cisplatin *in vitro* and *vivo*.

2. Results and discussion

2.1. Synthesis

The 11 new quinoline-coumarin derivatives, namly 3-(2′-pyridyl)-8-methoxyl-coumarin (H-QC1), 3-(2′-pyridyl)-7-methoxyl-coumarin (H-QC2), 3-(2′-pyridyl)-6-chloro-coumarin (H-QC3), 3-(2′-quinolyl)-6-hydroxy-coumarin (H-QC4), 3-(2′-quinolyl)-6,8-dichloro-coumarin (H-QC5), 3-(2′-benzothiazolyl)-7-fluoro-coumarin (H-QC6), 3-(2′-benzothiazolyl)-7-dimethylamino-coumarin (H-QC7), 3-(2′-benzothiazolyl)-7-chloro-coumarin (H-QC8), 3-(2′-benzothiazolyl)-5,6-butadienyl-coumarin (H-QC9), 3-(2′-benzothiazolyl)-7-diethylamino-coumarin (H-QC10), and 3-(2′-quinolyl)-5,6-butadienyl-coumarin (H-QC11) were designed (seen in Schemes 1−3), starting from 2-pyridylacetonitrile, benzothiazole-2-acetonitrile and 2-(quinolin-2-yl)acetonitrile, very similar to the previously synthesis step of 3-(2′-benzimidazolyl) coumarins derivatives [26,35−46]. In addition, the reaction of quinoline-coumarin derivatives (H-QC1−H-QC11) with *cis*-$Pt(DMSO)_2Cl_2$ (1.0 mmol) in a 2/1 M ratio in refluxing CH_3OH (10.0 mL) for 12 h afforded reddish-brown complexes **Pt1**−**Pt11** in good yield (86.2%−94.0%). The chemical structures of quinoline-coumarin complex **Pt1**−**Pt11** were characterized by various spectral methods and single-crystal X-ray diffraction analyses (Figs. 1 and 2 and S1−S29). Moreover, **Pt4** and **Pt5** were stable in Tris-HCl buffer solution at 48.0 h by HPLC analysis (Figs. S28 and S29).

2.2. Crystal structures

Figs. 1 and 2 and S1−S5 represents that, in the **Pt1**−**Pt5**, the square-planar geometry around the four-coordinated Pt^{II} center atom and the selective coordination of H-QC1, H-QC2, H-QC3, H-QC4 and H-QC5 *via* the C and N atoms. The C−Pt and N−Pt bond distances are 1.963−2.013 Å and 2.005−2.054 Å, respectively (Table S1−S15), which were in agreement with previously reported organoplatinum(II) complexes [31,47−54]. In addition, the Pt(II) centers of **Pt6**−**Pt11** also adopt four coordinated square planar geometry (Fig. S1−S11 and Table S16−S33).

2.3. Cytotoxicity

The cytotoxicity of quinoline-coumarin derivatives (H-QC1−H-QC11) and their Pt(II) complexes **Pt1**−**Pt11** against human A549 lung cells, drug resistance (cisplatin-resistant) of A549/DDP lung cells, SK-OV-3 ovarian cells, cisplatin-resistance SK-OV-3 ovarian cells (SK-OV-3/DDP), HeLa cervical carcinoma cells, non-small NCI−H460 lung cells, as well as against HL-7702 nontumorous cells were evaluated by MTT assay *in vitro*. **Pt1**−**Pt11** exhibited significantly enhanced antineoplastic activity in comparision to *cis*-$Pt(DMSO)_2Cl_2$, and quinoline-coumarin derivatives (H-QC1−H-QC11) in general. In addition, the new quinoline-coumarin derivatives complexes **Pt1**−**Pt11** display a highly promising antineoplastic activity. All the quinoline-coumarin derivatives complexes **Pt1**−**Pt11** inhibit the growth of the cisplatin-resistant of A549/DDP lung cells and HeLa cervical carcinoma cells at low nanomole concentrations (or micromole concentrations), with IC_{50} values as low as 100 nM−10.33 μM, and were more promising than cisplatin (75.02 ± 1.18 μM for A549/DDP or 12.09 ± 0.24 μM for HeLa) and other previously reported coumarin derivatives metal complexes [35−46]. The different antineoplastic activity for quinoline-coumarin derivatives complexes **Pt1**−**Pt11** were in the following order: **Pt4** > **Pt5** > **Pt1** > **Pt2** > **Pt3** > **Pt11** > **Pt9** > **Pt10** > **Pt7** > **Pt6** > **Pt8** > cisplatin. In all cases, the new quinoline-coumarin derivatives complexes **Pt1**−**Pt11** show selectivity toward A549/DDP lung cells and HeLa cervical carcinoma cells over the other

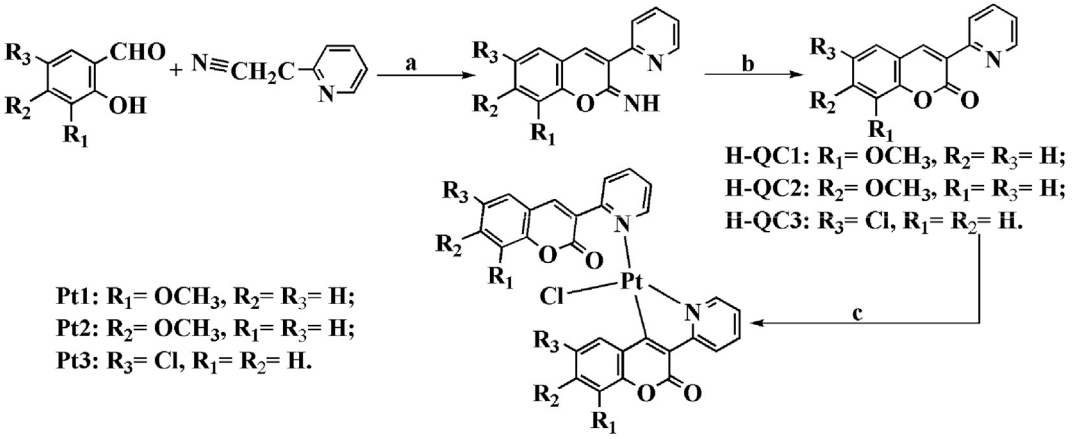

Scheme 1. Synthetic routes for coumarin derivatives ligands (H-QC1, H-QC2, H-QC3) and their Pt(II) complexes **Pt1**−**Pt3**. Reagents are the following: (a) EtOH, piperidine, 65 °C, 2.5 h; (b) 2.5% HCl, H_2O, 95 °C, 6.0 h; (c) *cis*-$Pt(DMSO)_2Cl_2$, CH_3OH, refluxing, 12 h.

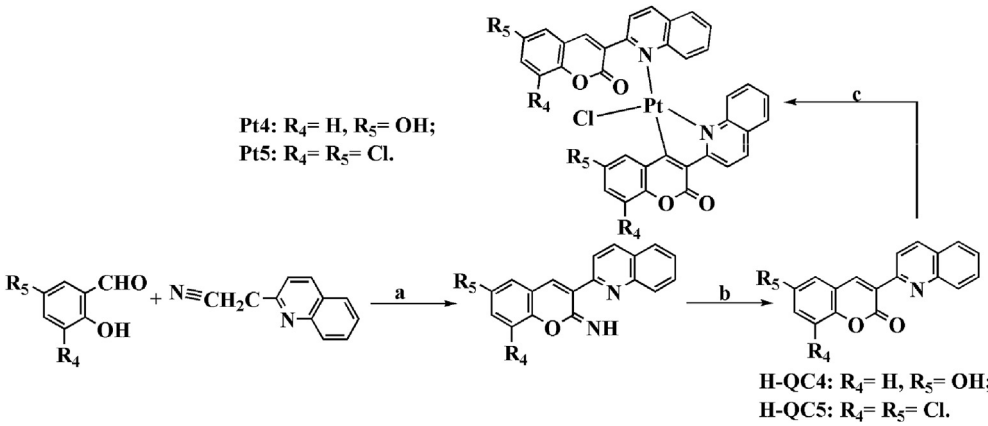

Scheme 2. Synthetic routes for quinoline-coumarin derivatives ligands (H-QC4, H-QC5) and their Pt(II) complexes **Pt4** and **Pt5**. Reagents are the following: (a) EtOH, piperidine, 65 °C, 2.5 h; (b) 2.5% HCl, H_2O, 95 °C, 6.0 h; (c) *cis*-Pt(DMSO)$_2$Cl$_2$, CH_3OH, refluxing, 12 h.

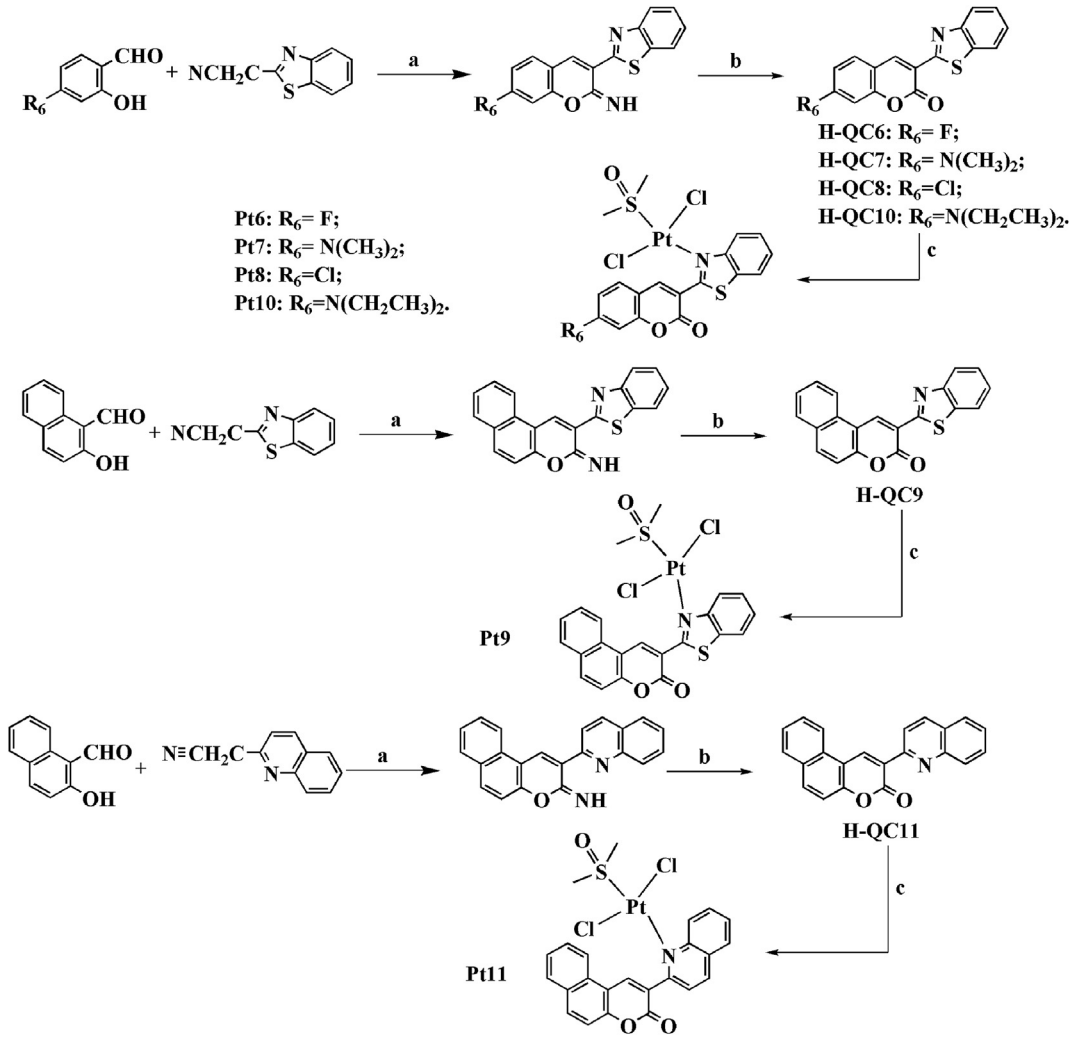

Scheme 3. Synthetic routes for coumarin derivatives ligands (H-QC6–H-QC11) and their Pt(II) complexes **Pt6**–**Pt11**. Reagents are the following: (a) EtOH, piperidine, 65 °C, 2.5 h; (b) 2.5% HCl, H_2O, 95 °C, 6.0 h; (c) *cis*-Pt(DMSO)$_2$Cl$_2$, CH_3OH, refluxing, 12.0 h.

cancer cells and nontumorous HL-7002 cell line ($IC_{50} > 150\ \mu M$). Because of the experimental group contained 1% DMSO solution, thus the vehicle group solution (including 1.0% DMSO) as another positive control. As shown in Table 1, the vehicle group solution (1.0% DMSO) showed low inhibitory rates against human cells, suggesting that it has no effect on cell growth and was suitable for control.

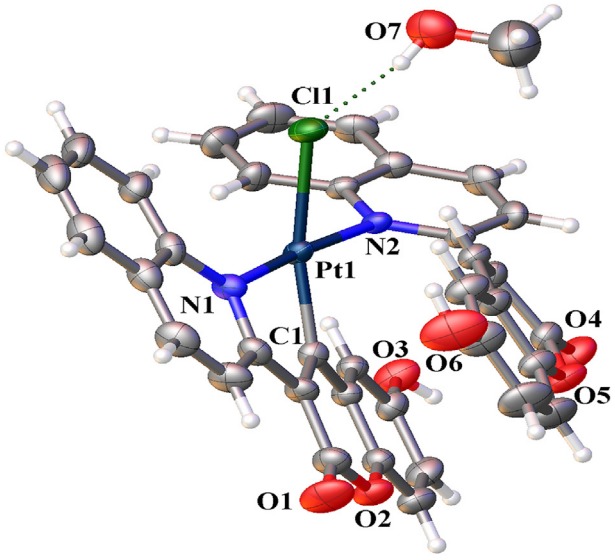

Fig. 1. Molecular structures of **Pt4**.

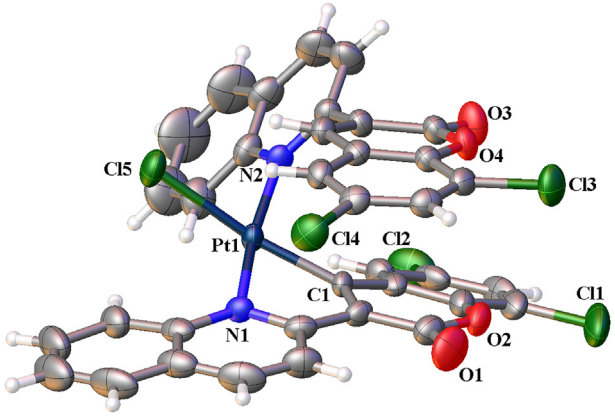

Fig. 2. Molecular structures of **Pt5**.

2.4. Cellular uptake

To confirm the location of two new organoplatinum(II) complexes within the A549/DDP cells, colocalization (confocal microscopy) studies of quinoline-coumarin derivatives complexes **Pt4** (100 nM) and **Pt5** (250 nM) with commercially available Mito-Red (red), which a mitochondria membrane imaging agent. Confocal microscopy assays suggested that quinoline-coumarin derivatives complexes **Pt4** (100 nM) and **Pt5** (250 nM) exhibited 525–530 nm emission (λ_{em}) in A549/DDP cells by ambient conditions upon excitation (λ_{ex}) at 490–495 nm (Fig. 3), which maybe acted as a green-colored luminescent agents for cellular applications. In addition, the results showed that the staining effect of quinoline-coumarin derivatives complexes **Pt4** (100 nM) and **Pt5** (250 nM) on mitochondria membrane was similar to that of mito-red (Fig. 3). Then, further than that, quinoline-coumarin derivatives complexes **Pt4** (100 nM) and **Pt5** (250 nM) could be effectively taken up by A549/DDP cells and were mainly retained (or accumulated) within the mitochondria membrane fraction, lossed of mitochondrial membrane potential (MMP) and targeted-mitochondria after 24.0 h of incubation (Fig. 3) and, thereby induced mitochondria damage and apoptosis [47–68].

2.5. Mitochondria dysfunction

Besides this, the increase in the cytochrome *c* (cyt *c*), caspases-3, apaf-1 and caspase-9 activity in quinoline-coumarin derivatives complexes **Pt4** (100 nM)- and **Pt5** (250 nM)-treatmented cells, and a quantity of bcl-2 was decreased (Fig. 4) was in the following order: **Pt4** (100 nM) > **Pt5** (250 nM), indicating that quinoline-coumarin derivatives complexes **Pt4** (100 nM) and **Pt5** (250 nM) induce mitochondria-mediated apoptosis in A549/DDP cells.

2.6. Apoptosis induction in vitro and vivo

The apoptosis-causing properties of quinoline-coumarin derivatives complexes **Pt4** (100 nM) and **Pt5** (250 nM) in A549/DDP cells were checked by flow cytometry (FCM). Treating the cisplatin-resistant of A549/DDP lung cells with quinoline-coumarin derivatives complexes **Pt4** (100 nM) and **Pt5** (250 nM) for 24.0 h (Fig. 5A–C), the amount of late (UR) and early (LR) apoptotic cells were 18.70% and 69.64%, and 63.21% and 10.66%, respectively.

Considering the cytotoxicity *in vitro*, we assessed the anti-tumor activity of quinoline-coumarin derivatives complexes **Pt4** against HeLa xenograft *in vivo* (Fig. 5C–D and Table S34–S36). The vehicle (5% DMSO in saline, v/v), and quinoline-coumarin complex **Pt4** (2.0 mg/kg per 2 days) (n = 6) were injected when the tumor volume grew to 200–400 mm^3. As shown in Fig. 5C–D and Table S34–S36, the effect of treated with quinoline-coumarin complex **Pt4** (37.2%) was higher than that of observed for cisplatin (2.0 mg/kg per 2 days, 35.2%) [69–86]. The tumor volume decreases by 42.7% after quinoline-coumarin complex **Pt4** treatment. There was no xenograft mouse death or obvious body weight loss under these conditions (Fig. 5C–D and Table S34–S36), indicating that quinoline-coumarin complex **Pt4** have no serious side effects.

3. Conclusion

Novel organoplatinum(II) complexes **Pt1**–**Pt11** with quinoline-coumarin derivatives (H-QC1–H-QC11) were first described. **Pt1**–**Pt11** were more selective for A549/DDP cells and HeLa cervical carcinoma cells (IC_{50} = 100 nM–10.33 μM) in comparision to other selected cells, and interestingly, they were considerably less cytotoxic to HL-7002 nontumorous cells (IC_{50} > 150 μM). The presence or absence of different 3-substituted groups in coumarin derivatives in organoplatinum(II) complexes, and thereby leading to differences in anti-tumor activity were in the following order: **Pt4** > **Pt5** > **Pt1** > **Pt2** > **Pt3** > **Pt11** > **Pt9** > **Pt10** > **Pt7** > **Pt6** > **Pt8** > cisplatin, whereas the 3-(2′-quinolyl)-6,8-dichloro-hydroxy-coumarin (H-QC5) ligand appears to significantly enhance the antineoplastic properties of the coumarin-modified organoplatinum(II) complexes. In addition, **Pt4** and **Pt5** display a green-colored luminescent properties, targeted mitochondrial and, thereby induced mainly mitochondria-mediated cell apoptosis. The quinoline-coumarin complex **Pt4** also showed potent *in vivo* anti-tumor effect after 21.0 days-treated. Therefore, the superior cytotoxicity and selectivity for coumarin organoplatinum(II) complexes **Pt1**–**Pt11** in comparison to cisplatin were further developed as some of Pt-based complexes.

4. Experimental methods

4.1. Synthesis of the quinoline-coumarin derivatives ligands

The 11 quinoline-coumarin derivatives (H-QC1–H-QC11)

Table 1
Cytotoxicity (IC_{50}±SD, μM) of quinoline-coumarin derivatives (H-QC1−H-QC11) and their Pt(II) complexes **Pt1**−**Pt11** following incubation for 24 h with select the cell lines.

compounds	A549	A549/DDP	SK-OV-3	HeLa	SK-OV-3/DDP	NCI−H460	HL-7702
H-QC1	>150	>150	>150	>150	>150	>150	>150
H-QC2	>150	>150	>150	>150	>150	>150	>150
H-QC3	>150	>150	>150	>150	>150	>150	>150
Pt1	>100	0.54 ± 0.14	>100	1.05 ± 0.72	>100	>100	>150
Pt2	>100	1.02 ± 0.35	>100	2.19 ± 1.02	>100	>100	>150
Pt3	>100	1.94 ± 0.76	>100	3.58 ± 0.83	>100	>100	>150
H-QC4	>100	>100	>100	>100	>100	>100	>150
H-QC5	>100	>100	>100	>100	>100	>100	>150
Pt4	35.22 ± 0.45	0.10 ± 0.05	75.25 ± 1.51	0.15 ± 0.09	58.41 ± 0.39	18.09 ± 0.54	>150
Pt5	50.78 ± 1.33	0.25 ± 0.11	91.08 ± 1.01	0.32 ± 0.14	70.01 ± 0.94	34.51 ± 0.19	>150
H-QC6	>150	>150	>150	>150	>150	>150	>150
P6	>100	8.01 ± 1.88	>100	8.86 ± 0.56	>100	>100	>150
H-QC7	>150	>150	>150	>150	>150	>150	>150
Pt7	>100	6.55 ± 0.19	>100	6.97 ± 1.11	>100	>100	>150
H-QC8	>150	>150	>150	>150	>150	>150	>150
Pt8	>100	10.27 ± 1.23	>100	10.33 ± 0.73	>100	>100	>150
H-QC9	>150	>150	>150	>150	>150	>150	>150
Pt9	>100	3.68 ± 0.84	>100	4.53 ± 1.09	>100	67.98 ± 1.99	>150
H-QC10	>150	>150	>150	>150	>150	>150	>150
Pt10	>100	5.97 ± 1.06	>100	6.30 ± 1.58	>100	>100	>150
H-QC11	>100	>100	>100	>100	>100	>100	>150
Pt11	>100	2.99 ± 0.41	>100	3.99 ± 0.15	>100	59.03 ± 0.83	>150
cis-$PtCl_2(DMSO)_2$	>150	>150	>150	>150	>150	>150	>150
vehicle group (1.0% DMSO)	>150	>150	>150	>150	>150	>150	>150
cisplatin	13.99 ± 1.033	75.02 ± 1.18	15.33 ± 1.78	12.09 ± 0.24	81.25 ± 1.03	12.89 ± 1.29	19.33 ± 0.24

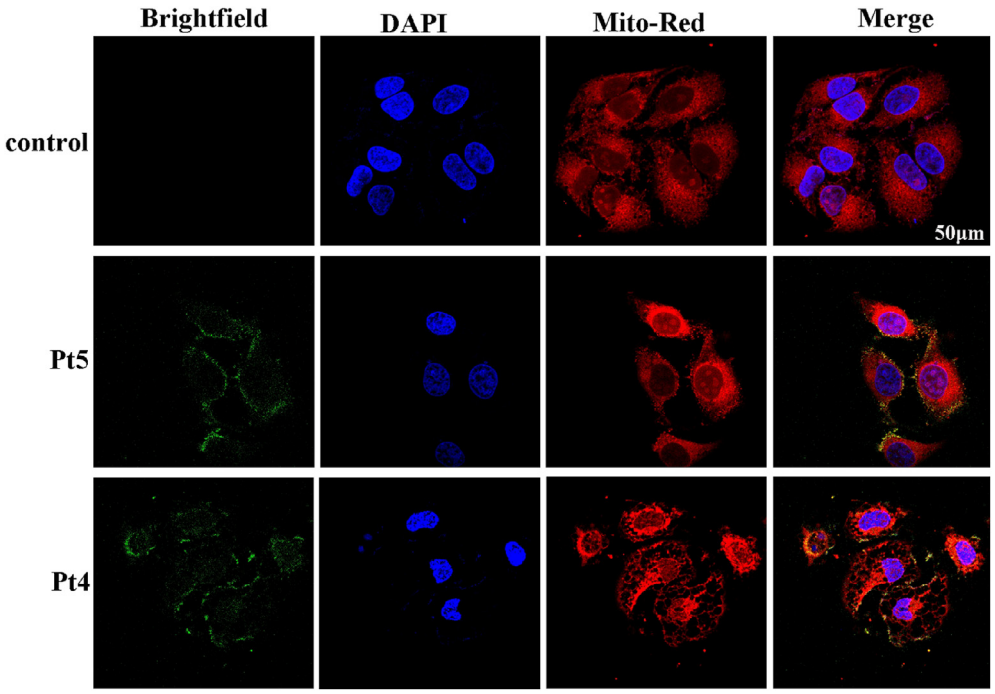

Fig. 3. Confocal microscopy imaging of A549/DDP cells incubated with quinoline-coumarin derivatives complexes **Pt4** (100 nM) and **Pt5** (250 nM) for 24.0 h, and then processed for Mito-Red (red, 500 nM) and the nuclei were stained with DAPI (blue). Quinoline-coumarin derivatives complexes **Pt4** and **Pt5**: λ_{em} = 525−530 nm, λ_{ex} = at 490−495 nm. (For interpretation of the references to color in this figure legend, the reader is referred to the Web version of this article.)

ligands were designed (seen in Schemes 1–3), starting from 2-pyridylacetonitrile, benzothiazole-2-acetonitrile and 2-(quinolin-2-yl)acetonitrile, very similar to the previously synthesis step of coumarin derivatives [35–46].

4.1.1. Synthesis of Pt1−Pt11

The reaction of H-QC1−H-QC11 with *cis*-$Pt(DMSO)_2Cl_2$ (1.0 mmol) in a 2/1 M ratio in refluxing CH_3OH (10.0 mL) for 12.0 h afforded reddish-brown complexes **Pt1**−**Pt11** in good yield (86.2%−94.0%).

*4.1.1.1. Data for **Pt1**.* Yield: 86.2%. Elemental analysis: calcd (%) for $C_{31}H_{25}ClN_2O_6Pt$: C 49.51, H 3.35, N 3.72; found: C 49.49, H 3.38, N 3.70. IR (KBr): 3429, 2939, 1727, 1713, 1696, 1601, 1577, 1475, 1348, 1276, 1096, 961, 793, 771, 554 cm^{-1}. ESI-MS: m/z = 462.5 for $[QC1+Pt]^+$.

*4.1.1.2. Data for **Pt2**.* Yield: 94.0%. Elemental analysis: calcd (%) for

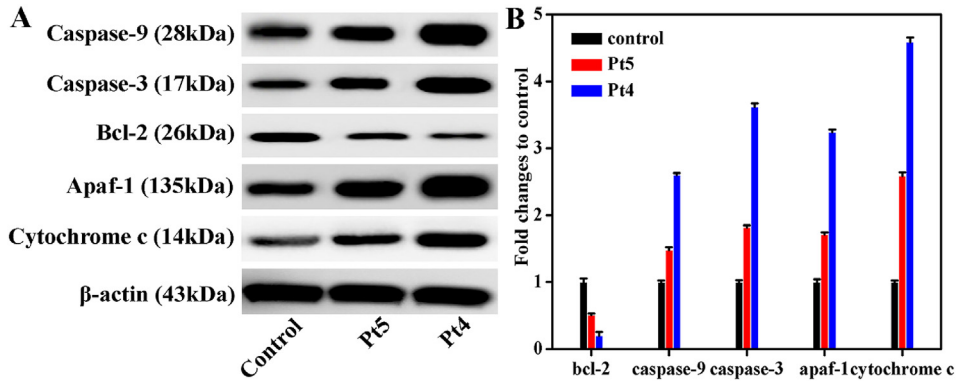

Fig. 4. Western blot images (A) and analysis (B) of certain apoptosis proteins in A549/DDP cells for 24.0 h incubation with quinoline-coumarin derivatives complexes **Pt4** (100 nM) and **Pt5** (250 nM).

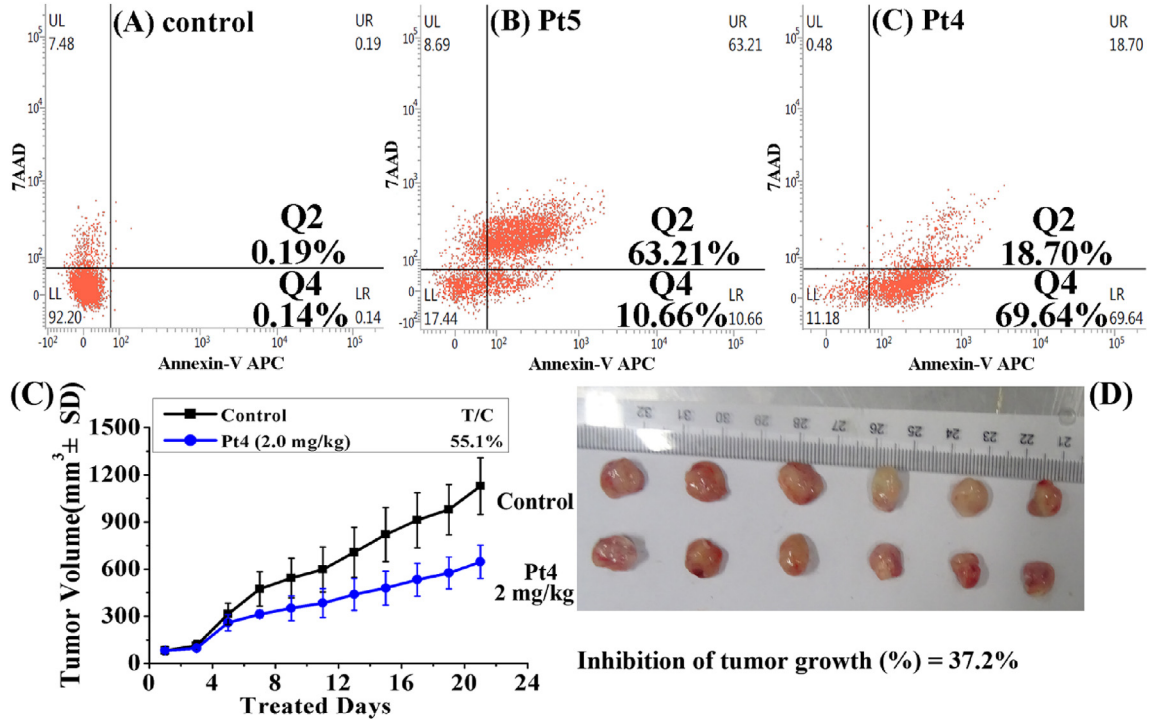

Fig. 5. Quinoline-coumarin derivatives Pt complexes caused cancer cell apoptosis *in vitro* and *vivo*. (A–C) The quinoline-coumarin derivatives complexes **Pt4** (100 nM) and **Pt5** (250 nM) induces apoptosis in A549/DDP cells for 24 h, and the cells stains by Annexin-V APC (Ex/Em = 633 nm/660 nm) and 7AAD (red, Ex/Em = 546 nm/647 nm) staining, and checked by FCM. (C and D) The growth and photographs of HeLa tumor xenograft after treated with quinoline-coumarin complex **Pt4** (2.0 mg/kg per 2 days) (n = 6). (For interpretation of the references to color in this figure legend, the reader is referred to the Web version of this article.)

$C_{31}H_{25}ClN_2O_6Pt$: C 49.51, H 3.35, N 3.72; found: C 49.50, H 3.37, N 2.69. IR (KBr): 3433, 1725, 1698, 1604, 1477, 1461, 1369, 1277, 1218, 1127, 1027, 832, 788, 758, 524 cm^{-1}. ESI-MS: m/z = 518.3 for $[QC2+Pt + Cl + H_2O-H]^-$. ^1H NMR (500 MHz, DMSO-d_6) δ 9.30 (d, J = 5.9 Hz, 1H), 8.87 (s, 2H), 8.69 (d, J = 4.9 Hz, 2H), 8.27 (d, J = 8.0 Hz, 2H), 7.92–7.86 (m, 4H), 7.09 (d, J = 2.4 Hz, 2H), 7.02 (dd, J = 8.6, 2.5 Hz, 2H), 3.90 (s, 6H).

4.1.1.3. Data for ***Pt3****.* Yield: 90.3%. Elemental analysis: calcd (%) for $C_{29}H_{19}Cl_3N_2O_4Pt$: C 45.78, H 2.52, N 3.68; found: C 45.76, H 2.55, N 3.67. IR (KBr): 3450, 3086, 1732, 1705, 1598, 1565, 1482, 1351, 1233, 1129, 1082, 990, 837, 792, 695, 575 cm^{-1}. ESI-MS: m/z = 542.7 for $[QC3+Pt+2Cl]^-$. ^1H NMR (500 MHz, DMSO-d_6) δ 9.35 (d, J = 6.1 Hz, 1H), 8.86 (s, 1H), 8.71 (d, J = 4.7 Hz, 1H), 8.29 (d, J = 8.0 Hz, 1H), 7.92 (dd, J = 8.5, 6.6 Hz, 1H), 7.49 (dd, J = 7.2, 1.9 Hz, 1H), 7.38–7.34 (m, 2H).

4.1.1.4. Data for ***Pt4****.* Yield: 87.6%. Elemental analysis: calcd (%) for $C_{37}H_{25}ClN_2O_6Pt$: C 53.92, H 3.06, N 3.40; found: C 53.90, H 3.10, N 3.38. IR (KBr): 3434, 3035, 3010, 2917, 1627, 1402, 1302, 1156, 1133, 1020, 982, 941, 736, 691, 431 cm^{-1}. ESI-MS: m/z = 522.2 for $[QC4+Pt + Cl-H]^-$. ^1H NMR (500 MHz, DMSO-d_6) δ 8.84 (s, 2H), 8.72 (s, 1H), 8.33 (d, J = 8.7 Hz, 2H), 8.22 (d, J = 8.5 Hz, 2H), 8.15 (d, J = 8.1 Hz, 2H), 7.97–7.92 (m, 2H), 7.76 (t, J = 7.5 Hz, 2H), 7.39 (d, J = 8.8 Hz, 2H), 7.28 (d, J = 2.8 Hz, 2H), 7.18 (dd, J = 8.9, 2.9 Hz, 2H).

4.1.1.5. Data for ***Pt5****.* Yield: 89.1%. Elemental analysis: calcd (%) for $C_{37}H_{21}Cl_5N_2O_4Pt$: C 47.79, H 2.28, N 3.01; found: C 47.75, H 2.30, N 2.26. IR (KBr): 3427, 3013, 1721, 1566, 1508, 1215, 1144, 1025, 960, 832, 752, 505, 436 cm^{-1}. ESI-MS: m/z = 606.1 for $[QC5+Pt+2Cl]^-$.

^{1}H NMR (500 MHz, DMSO-d_6) δ 8.88 (s, 2H), 8.72 (d, J = 2.5 Hz, 1H), 8.60 (dd, J = 8.9, 4.3 Hz, 2H), 8.51 (d, J = 8.6 Hz, 2H), 8.26 (d, J = 8.6 Hz, 2H), 8.16 (d, J = 2.4 Hz, 2H), 8.11 (d, J = 8.5 Hz, 2H), 7.69 (dt, J = 11.8, 7.0 Hz, 4H).

4.1.1.6. Data for ***Pt6***. Yield: 86.9%. Elemental analysis: calcd (%) for $C_{18}H_{14}Cl_2FNO_3PtS_2$: C 33.71, H 2.20, N 2.18; found: C 33.69, H 2.25, N 2.17. ^{1}H NMR (500 MHz, DMSO-d_6) δ 9.28 (s, 1H), 8.19 (dd, J = 9.5, 6.8 Hz, 2H), 8.09 (d, J = 8.1 Hz, 1H), 7.58 (ddd, J = 9.5, 7.9, 4.8 Hz, 2H), 7.54–7.47 (m, 1H), 7.40 (td, J = 8.8, 2.5 Hz, 1H), 3.33 (s, 6H).

4.1.1.7. Data for ***Pt7***. Yield: 91.1%. Elemental analysis: calcd (%) for $C_{20}H_{20}Cl_2N_2O_3PtS_2$: C 36.04, H 3.02, N 4.20; found: C 36.02, H 3.05, N 4.17. ^{1}H NMR (500 MHz, DMSO-d_6) δ 9.06 (s, 1H), 8.13 (d, J = 8.1 Hz, 1H), 8.00 (d, J = 8.4 Hz, 1H), 7.82 (d, J = 8.9 Hz, 1H), 7.53 (t, J = 7.7 Hz, 1H), 7.42 (t, J = 7.5 Hz, 1H), 6.91–6.86 (m, 1H), 6.70 (d, J = 2.2 Hz, 1H), 3.12 (s, 6H).

4.1.1.8. Data for ***Pt8***. Yield: 85.7%. Elemental analysis: calcd (%) for $C_{18}H_{14}Cl_3NO_3PtS_2$: C 32.86, H 2.14, N 2.13; found: C 32.84, H 2.15, N 2.10. ^{1}H NMR (500 MHz, DMSO-d_6) δ 8.97 (s, 1H), 8.82 (d, J = 8.8 Hz, 1H), 8.44 (d, J = 8.8 Hz, 1H), 8.27 (d, J = 8.5 Hz, 1H), 8.17 (d, J = 8.1 Hz, 1H), 7.98 (t, J = 7.8 Hz, 1H), 7.78 (t, J = 7.5 Hz, 1H), 7.70 (d, J = 8.9 Hz, 1H), 3.13 (s, 6H).

4.1.1.9. Data for ***Pt9***. Yield: 89.0%. Elemental analysis: calcd (%) for $C_{22}H_{17}Cl_2NO_3PtS_2$: C 39.23, H 2.54, N 2.08; found: C 39.20, H 2.58, N 2.06. ^{1}H NMR (500 MHz, DMSO-d_6) δ 9.86 (s, 1H), 8.74 (d, J = 8.4 Hz, 1H), 8.37 (d, J = 9.1 Hz, 1H), 8.24–8.14 (m, 4H), 7.86 (t, J = 7.7 Hz, 2H), 7.62 (t, J = 7.7 Hz, 1H), 7.52 (t, J = 7.5 Hz, 1H), 3.17 (s, 6H).

4.1.1.10. Data for ***Pt10***. Yield: 93.5%. Elemental analysis: calcd (%) for $C_{22}H_{24}Cl_2N_2O_3PtS_2$: C 38.04, H 3.48, N 4.03; found: C 38.02, H 3.53, N 4.01. ^{1}H NMR (500 MHz, DMSO-d_6) δ 9.03 (s, 1H), 8.12 (d, J = 7.9 Hz, 1H), 7.99 (d, J = 8.1 Hz, 1H), 7.79 (d, J = 9.0 Hz, 1H), 7.57–7.50 (m, 1H), 7.45–7.38 (m, 1H), 6.86 (dd, J = 8.9, 2.4 Hz, 1H), 6.68 (d, J = 2.4 Hz, 1H), 3.52 (q, J = 7.0 Hz, 4H), 1.17 (t, J = 7.0 Hz, 6H).

4.1.1.11. Data for ***Pt11***. Yield: 87.0%. Elemental analysis: calcd (%) for $C_{24}H_{19}Cl_2NO_3PtS$: C 43.19, H 2.87, N 2.10; found: C 43.17, H 2.90, N 2.11. ^{1}H NMR (500 MHz, DMSO-d_6) δ 10.03 (s, 1H), 9.79 (d, J = 8.7 Hz, 1H), 8.86 (d, J = 8.5 Hz, 1H), 8.51 (d, J = 3.5 Hz, 1H), 8.38 (d, J = 3.2 Hz, 1H), 8.06 (d, J = 8.5 Hz, 1H), 7.90 (t, J = 7.6 Hz, 1H), 7.86–7.80 (m, 2H), 7.77 (d, J = 9.0 Hz, 1H), 7.68 (d, J = 8.7 Hz, 2H), 3.06 (s, 6H).

4.1.2. The other experimental methods

The X-Ray crystallography structures of quinoline-coumarin derivatives organoplatinum(II) complexes **Pt1**–**Pt11** were refined by SHELX-97 programs [87,88]. The experimental steps for antitumor activities of quinoline-coumarin organoplatinum(II) complexes **Pt1**–**Pt11** were similar to those illustrated in Galons, Barraja, Georg and Chao et al. [25,69–86].

Acknowledgments

This work was supported by the National Natural Science Foundation of China (Nos. 21867017 and 21761033), the Natural Science Foundation of Guangxi (No. 2018GXNSFBA138021, 2018GXNSFBA281188 and 2016GXNSFAA380300), the China University Students Innovative Project (No. 201910606139) as well as the Innovative Team & Outstanding Talent Program of Colleges and Universities in Guangxi (2014-49 and 2017–38).

Appendix A. Supplementary data

Supplementary data to this article can be found online at https://doi.org/10.1016/j.ejmech.2019.111751.

References

[1] J. Zhao, D. Zhang, W. Hua, W. Li, G. Xu, S. Gou, Anticancer activity of bifunctional organometallic Ru(II) arene complexes containing a 7-hydroxycoumarin group, Organometallics 37 (2018) 441–447.
[2] Y. Yang, L. Guo, Z. Tian, X. Ge, Y. Gong, H. Zheng, S. Shi, Z. Liu, Lysosome-targeted phosphine-imine half-sandwich iridium(III) anticancer complexes: synthesis, characterization, and biological activity, Organometallics 38 (2019) 1761–1769.
[3] T.C. Johnstone, K. Suntharalingam, S.J. Lippard, The next generation of platinum drugs: targeted Pt(II) agents, nanoparticle delivery, and Pt(IV) prodrugs, Chem. Rev. 116 (2016) 3436–3486.
[4] N.J. Wheate, S. Walker, G.E. Craig, R. Oun, The status of platinum anticancer drugs in the clinic and in clinical trials, Dalton Trans. 39 (2010) 8113–8127.
[5] L. Kelland, The resurgence of platinum-based cancer chemotherapy, Nat. Rev. Cancer 7 (2007) 573–584.
[6] M. Galanski, B.K. Keppler, Searching for the magic bullet: anticancer platinum drugs which can be accumulated or activated in the tumor tissue, Anti-Cancer Agents Med. Chem. 7 (2007) 55–73.
[7] T.W. Hambley, Metal-based therapeutics, Science 318 (2007) 1392–1393.
[8] D. Wang, S.J. Lippard, Cellular processing of platinum anticancer drugs, Nat. Rev. Drug Discov. 4 (2005) 307–320.
[9] X. Wang, X. Wang, S. Jin, N. Muhammad, Z. Guo, Stimuliresponsive therapeutic metallodrugs, Chem. Rev. 119 (2019) 1138–1192.
[10] Z. Liu, I. Romero-Canelón, B. Qamar, J.M. Hearn, A. Habtemariam, N.P.E. Barry, A.M. Pizarro, G.J. Clarkson, P.J. Sadler, The potent oxidant anticancer activity of organoiridium catalysts, Angew. Chem. Int. Ed. 53 (2014) 3941–3946.
[11] A. Zamora, S.A. Pérez, M. Rothemund, V. Rodríguez, R. Schobert, C. Janiak, J. Ruiz, Exploring the influence of the aromaticity on the anticancer and antivascular activities of organoplatinum(II) complexes, Chem. Eur J. 23 (2017) 5614–5625.
[12] R. Rubbiani, I. Kitanovic, H. Alborzinia, S. Can, A. Kitanovic, L.A. Onambele, M. Stefanopoulou, Y. Geldmacher, W.S. Sheldrick, G. Wolber, A. Prokop, S. Wölfl, I. Ott, Benzimidazol-2-ylidene gold(I) complexes are thioredoxin reductase inhibitors with multiple antitumor properties, J. Med. Chem. 53 (2010) 8608–8618.
[13] X. Ma, J. Jia, R. Cao, X. Wang, H. Fei, Histidine-iridium(III) coordination-based peptide luminogenic cyclization and cyclo-RGD peptides for cancer-cell targeting, J. Am. Chem. Soc. 136 (2014) 17734–17737.
[14] J.P. Luzio, P.R. Pryor, N.A. Bright, Lysosomes: fusion and function, Nat. Rev. Mol. Cell Biol. 8 (2007) 622–632.
[15] P. Saftig, J. Klumperman, Lysosome biogenesis and lysosomal membrane proteins: trafficking meets function, Nat. Rev. Mol. Cell Biol. 10 (2009) 623–635.
[16] L. He, C.-P. Tan, R.-R. Ye, Y.-Z. Zhao, Y.-H. Liu, Q. Zhao, L.-N. Ji, Z.-W. Mao, Theranostic iridium(III) complexes as one- and twophoton phosphorescent trackers to monitor autophagic lysosomes, Angew. Chem. Int. Ed. 53 (2014) 12137–12141.
[17] M.A. Jakupec, M. Galanski, V.B. Arion, C.G. Hartinger, B.K. Keppler, Antitumour metal compounds: more than theme and variations, Dalton Trans. (2008) 183–194.
[18] A.M. Thayer, Platinum drugs take their roll, Chem. Eng. News 88 (2010) 24–28.
[19] R. Pettinari, F. Marchetti, F. Condello, C. Pettinari, G. Lupidi, R. Scopelliti, S. Mukhopadhyay, T. Riedel, P.J. Dyson, Ruthenium(II)-arene RAPTA type complexes containing curcumin and bisdemethoxycurcumin display potent and selective anticancer activity, Organometallics 33 (2014) 3709–3715.
[20] G. Gasser, I. Ott, N. Metzler-Nolte, Organometallic anticancer complexes, J. Med. Chem. 54 (2011) 3–25.
[21] M. Frik, J. Fernández-Gallardo, O. Gonzalo, V. Mangas-Sanjuan, M. González-Alvarez, A.S. del Valle, C. Hu, I. González-Alvarez, M. Bermejo, I. Marzo, M. Contel, Cyclometalated iminophosphorane gold(III) and platinum(II) complexes. A highly permeable cationic platinum(II) compound with promising anticancer properties, J. Med. Chem. 58 (2015) 5825–5841.
[22] S. Medici, M. Peana, V.M. Nurchi, J.I. Lachowicz, G. Crisponi, M.A. Zoroddu, Noble metals in medicine: latests advances, Coord. Chem. Rev. 284 (2015) 329–350.
[23] C. Cullinane, G.B. Deacon, P.R. Drago, T.W. Hambley, K.T. Nelson, L.K. Webster, Preparation and cell growth inhibitory activity of $[PtR_2L_2]$ (R=polyfluorophenyl, L_2=diene, cyclohexane-1,2-diamine (chxn) or *cis*-(dimethyl sulfoxide)$_2$) and the X-ray crystal structure of $[Pt(C_6F_5)_2(cis\text{-}chxn)]$, J. Inorg. Biochem. 89 (2002) 293–301.
[24] W. Liu, R. Gust, Metal N-heterocyclic carbene complexes as potential antitumor metallodrugs, Chem. Soc. Rev. 42 (2013) 755–773.
[25] Z.-F. Chen, Q.-P. Qin, J.-L. Qin, Y.-C. Liu, K.-B. Huang, Y.-L. Li, T. Meng, G.-H. Zhang, Y. Peng, X.-J. Luo, H. Liang, Stabilization of G-quadruplex DNA, inhibition of telomerase activity, and tumor cell apoptosis by organoplatinum(II) complexes with oxoisoaporphine, J. Med. Chem. 58 (2015)

2159–2179.
[26] Q.-P. Qin, S.-L. Wang, M.-X. Tan, Z.-F. Wang, X.-L. Huang, Q.-M. Wei, B.-B. Shi, B.-Q. Zou, H. Liang, Synthesis and antitumor mechanisms of two novel platinum(II) complexes with 3-(2′-benzimidazolyl)-7-methoxycoumarin, Metall 10 (2018) 1160–1169.
[27] I.V. Grishagin, J.B. Pollock, S. Kushal, T.R. Cook, P.T. Stang, B.Z. Olenyuk, *In vivo* anticancer activity of rhomboidal Pt(II) metallacycles, Proc. Natl. Acad. Sci. U.S.A. 111 (2014) 18448–18453.
[28] A. Zamora, S.A. Perez, V. Rodriguez, C. Janiak, G.S. Yellol, J. Ruiz, On the Dual antitumor and anti-angiogenic activity of organoplatinum(II) complexes, J. Med. Chem. 58 (2015) 1320–1336.
[29] K. Butsch, S. Elmas, N.S. Gupta, R. Gust, F. Heinrich, A. Klein, Y. von Mering, M. Neugebauer, I. Ott, M. Schafer, H. Scherer, T. Schurr, Organoplatinum(II) and -palladium(II) complexes of nucleobases and their derivatives, Organometallics 28 (2009) 3906–3915.
[30] A. Klein, T. Schurr, H. Scherer, N.S. Gupta, Cytosine binding in the novel organoplatinum(II) Complex [(COD)PtMe(cytosine)]-(SbF_6), Organometallics 26 (2007) 230–233.
[31] A. Luning, J. Schur, L. Hamel, I. Ott, A. Klein, Strong cytotoxicity of organometallic platinum complexes with alkynyl ligands, Organometallics 32 (2013) 3662–3672.
[32] T. Zou, J. Liu, C.T. Lum, C. Ma, R.C.-T. Chan, C.-N. Lok, W.-M. Kwok, C.-M. Che, Luminescent cyclometalated platinum(II) complex forms emissive intercalating adducts with double-stranded DNA and RNA: differential emissions and anticancer activities, Angew. Chem. Int. Ed. 53 (2014) 10119–10123.
[33] A. Zamora, S.A. Pérez, M. Rothemund, V. Rodríguez, R. Schobert, C. Janiak, J. Ruiz, Exploring the influence of the aromaticity on the anticancer and antivascular activities of organoplatinum(II) complexes, Chem. Eur J. 23 (2017) 5614–5625.
[34] S. Datta, S.K. Misra, M.L. Saha, N. Lahiri, J. Louie, D. Pan, P.J. Stang, Orthogonal self-assembly of an organoplatinum(II) metallacycle and cucurbit[8]uril that delivers curcumin to cancer cells, Proc. Natl. Acad. Sci. 115 (2018) 8087–8092.
[35] Q.-P. Qin, Z.-F. Wang, X.-L. Huang, M.-X. Tan, B.-B. Shi, H. Liang, High *in vitro* and *in vivo* tumor-selective novel ruthenium(II) complexes with 3-(2′-Benzimidazolyl)-7-fluoro-coumarin, ACS Med. Chem. Lett. 10 (2019) 936–940.
[36] T. Meng, Q.-P. Qin, Z.-R. Wang, L.-T. Peng, H.-H. Zou, Z.-Y. Gan, M.-X. Tan, K. Wang, F.-P. Liang, Synthesis and biological evaluation of substituted 3-(2′-benzimidazolyl) coumarin platinum(II) complexes as new telomerase inhibitors, J. Inorg. Biochem. 189 (2018) 143–150.
[37] K. Paul, S. Bindal, V. Luxami, Synthesis of new conjugated coumarin–benzimidazole hybrids and their anticancer activity, Bioorg. Med. Chem. Lett 23 (2013) 3667–3672.
[38] S. Cosconati, A. Rizzo, R. Trotta, B. Pagano, S. Iachettini, S. De Tito, I. Lauri, I. Fotticchia, M. Giustiniano, L. Marinelli, C. Giancola, E. Novellino, A. Biroccio, A. Randazzo, Shooting for selective drug-like G-quadruplex binders: evidence for telomeric DNA damage and tumor cell death, J. Med. Chem. 55 (2012) 9785–9792.
[39] S. Cosconati, L. Marinelli, R. Trotta, A. Virno, L. Mayol, E. Novellino, A.J. Olson, A. Randazzo, Tandem application of virtual screening and NMR experiments in the discovery of brand new DNA quadruplex groove binders, J. Am. Chem. Soc. 131 (2009) 16336–16337.
[40] W. Wu, W. Wu, S. Ji, H. Guo, J. Zhao, Accessing the long-lived emissive 3IL triplet excited states of coumarin fluorophores by direct cyclometallation and its application for oxygen sensing and upconversion, Dalton Trans. 40 (2011) 5953–5963.
[41] M. Ali, L. Dondaine, A. Adolle, C. Sampaio, F. Chotard, P. Richard, F. Denat, A. Bettaieb, P. Le Gendre, V. Laurens, C. Goze, C. Paul, E. Bodio, Anticancer agents: does a phosphonium behave like a gold(I) phosphine complex? Let a "smart" probe answer!, J. Med. Chem. 58 (2015) 4521–4528.
[42] H.S. Jung, P.S. Kwon, J.W. Lee, J.I. Kim, C.S. Hong, J.W. Kim, S. Yan, J.Y. Lee, J.H. Lee, T. Joo, J.S. Kim, Coumarin-derived Cu^{2+}-selective fluorescence sensor: synthesis, mechanisms, and applications in living cells, J. Am. Chem. Soc. 131 (2009) 2008–2012.
[43] R.M. Christie, C.H. Lui, Studies of fluorescent dyes: part 2. An investigation of the synthesis and electronic spectral properties of substituted 3-(2′-benzimidazolyl) coumarins, Dyes Pigments 47 (2000) 79–89.
[44] W. Wu, P. Yang, L. Ma, J. Lalevée, J. Zhao, Visible-light harvesting Pt^{II} complexes as singlet oxygen photosensitizers for photooxidation of 1,5-dihydroxynaphthalene, Eur. J. Inorg. Chem. (2013) 228–231.
[45] Ö. Şahin, Ü.Ö. Özdemir, N. Seferoğlu, Z.K. Genc, K. Kaya, B. Aydıner, S. Tekin, Z. Seferoğlu, New platinum(II) and palladium(II) complexes of coumarinthiazole Schiff base with a fluorescent chemosensor properties: synthesis, spectroscopic characterization, X-ray structure determination, in vitro anticancer activity on various human carcinoma cell lines and computational studies, J. Photochem. Photobiol., B 178 (2018) 428–439.
[46] I. Kostova, G. Momekov, New cerium(III) complexes of coumarins-synthesis, characterization and cytotoxicity evaluation, Eur. J. Med. Chem. 42 (2008) 178–188.
[47] M. Skander, P. Retailleau, B. Bourri, L. Schio, P. Mailliet, A. Marinetti, N-heterocyclic carbene-amine Pt(II) complexes, a new chemical space for the development of platinum-based anticancer drugs, J. Med. Chem. 53 (2010) 2146–2154.
[48] E. Chardon, G. Dahm, G. Guichard, S. Bellemin-Laponnaz, Derivatization of preformed platinum N-heterocyclic carbine complexes with amino acid and peptide ligands and cytotoxic activities toward human cancer cells, Organometallics 31 (2012) 7618–7621.
[49] A.A. Ali, H. Nimir, C. Aktas, V. Huch, U. Rauch, K.-H. Schäfer, M. Veith, Organoplatinum(II) complexes with 2-acetylthiophene thiosemicarbazone: synthesis, characterization, crystal structures, and *in vitro* antitumor activity, Organometallics 31 (2012) 2256–2262.
[50] M. Clemente, I.H. Polat, J. Albert, R. Bosque, M. Crespo, J. Granell, C. López, M. Martínez, J. Quirante, R. Messeguer, C. Calvis, J. Badía, L. Baldomà, M. Font-Bardia, M. Cascante, Platinacycles containing a primary amine platinum(II) compounds for treating cisplatin-resistant cancers by oxidant therapy, Organometallics 37 (2018) 3502–3514.
[51] M. Enders, B. Görling, A.B. Braun, J.E. Seltenreich, L.F. Reichenbach, K. Rissanen, M. Nieger, B. Luy, U. Schepers, S. Bräse, Cytotoxicity and NMR studies of platinum complexes with cyclooctadiene ligands, Organometallics 33 (2014) 4027–4034.
[52] M.-G. Mendoza-Ferri, C.G. Hartinger, R.E. Eichinger, N. Stolyarova, K. Severin, M.A. Jakupec, A.A. Nazarov, B.K. Keppler, Influence of the spacer length on the *in vitro* anticancer activity of dinuclear ruthenium-arene compounds, Organometallics 27 (2008) 2405–2407.
[53] M.E. Kelly, A. Dietrich, S. Gomez-Ruiz, B. Kalinowski, G.N. Kaluderovic, T. Muller, R. Paschke, J. Schmidt, D. Steinborn, C. Wagner, H. Schmidt, Platinum(IV) metallacrown ethers: synthesis, structures, host properties and anticancer evaluation, Organometallics 27 (2008) 4917–4927.
[54] J. Li, Z. Tian, X. Ge, Z. Xu, Y. Feng, Z. Liu, Design, synthesis, and evaluation of fluorine and naphthyridinee based half-sandwich organoiridium/ruthenium complexes with bioimaging and anticancer activity, Eur. J. Med. Chem. 163 (2019) 830–839.
[55] L. Zeng, P. Gupta, Y. Chen, E. Wang, L.-N. Ji, H. Chao, Z.-S. Chen, The development of anticancer ruthenium(II) complexes: from single molecule compounds to nanomaterials, Chem. Soc. Rev. 46 (2017) 5771–5804.
[56] Q.Q. Yu, Y.A. Liu, L. Xu, C.P. Zheng, F.L. Le, X.Y. Qin, Y.Y. Liu, J. Liu, Ruthenium(II) polypyridyl complexes: cellular uptake, cell image and apoptosis of HeLa cancer cells induced by double targets, Eur. J. Med. Chem. 82 (2014) 82–95.
[57] J. Liu, Y. Chen, G. Li, P. Zhang, C. Jin, L. Zeng, L. Ji, H. Chao, Ruthenium(II) polypyridyl complexes as mitochondria-targeted two-photon photodynamic anticancer agents, Biomaterials 56 (2015) 140–153.
[58] G.H. Zhang, J.M. Yuan, G. Qian, C.X. Gu, K. Wei, D.L. Mo, J.K. Qin, Y. Peng, Z.P. Zhou, C.X. Pan, G.F. Su, Phthalazino[1,2-b]quinazolinones as p53 activators: cell cycle arrest, apoptotic response and bak-bcl-xl complex reorganization in bladder cancer cells, J. Med. Chem. 60 (2017) 6853–6866.
[59] Q.-P. Qin, J.-L. Qin, T. Meng, W.-H. Lin, C.-H. Zhang, Z.-Z. Wei, J.-N. Chen, Y.-C. Liu, H. Liang, Z.-F. Chen, High *in vivo* antitumor activity of cobalt oxoisoaporphine complexes by targeting G-quadruplex DNA, telomerase and disrupting mitochondrial functions, Eur. J. Med. Chem. 124 (2016) 380–392.
[60] R.-R. Ye, C.-P. Tan, L. He, M.-H. Chen, L.-N. Ji, Z.-W. Mao, Cyclometalated Ir(III) complexes as targeted theranostic anticancer therapeutics: combining HDAC inhibition with photodynamic therapy, Chem. Commun. 50 (2014) 10945–10948.
[61] T. Meng, Q.-P. Qin, Z.-L. Chen, H.-H. Zou, K. Wang, F.-P. Liang, High in vitro and *in vivo* antitumor activities of Ln(III) complexes with mixed 5,7-dichloro-2-methyl-8-quinolinol and 4,4′-dimethyl-2,2′-bipyridyl chelating ligands, Eur. J. Med. Chem. 169 (2019) 103–110 (2019).
[62] Q.-P. Qin, Z.-F. Wang, S.-L. Wang, D.-M. Luo, B.-Q. Zou, P.-F. Yao, M.-X. Tan, H. Liang, *In vitro* and *in vivo* antitumor activities of three novel binuclear platinum(II) complexes with 4′-substituted-2,2′:6′,2″-terpyridine ligands, Eur. J. Med. Chem. 170 (2019) 195–202.
[63] C.-C. Zeng, S.-H. Lai, J.-H. Yao, C. Zhang, H. Yin, W. Li, B.-J. Han, Y.-J. Liu, The induction of apoptosis in HepG-2 cells by ruthenium(II) complexes through an intrinsic ROS-mediated mitochondrial dysfunction pathway, Eur. J. Med. Chem. 122 (2016) 118–126.
[64] G.C. Kujoth, A. Hiona, T.D. Pugh, S. Someya, K. Panzer, S.E. Wohlgemuth, T. Hofer, A.Y. Seo, R. Sullivan, W.A. Jobling, J.D. Morrow, H. Van Remmen, J.M. Sedivy, T. Yamasoba, M. Tanokura, R. Weindruch, C. Leeuwenburgh, T.A. Prolla, Mitochondrial DNA mutations, oxidative stress, and apoptosis in mammalian aging, Science 309 (2005) 481–484.
[65] T. Lu, Y. Pan, S.-Y. Kao, C. Li, I. Kohane, J. Chan, B.A. Yankner, Gene regulation and DNA damage in the ageing human brain, Nature 429 (2004) 883–891.
[66] V. Sharma, D. Anderson, A. Dhawan, Zinc oxide nanoparticles induce oxidative DNA damage and ROS-triggered mitochondria mediated apoptosis in human liver cells (HepG2), Apoptosis 17 (2012) 852–870.
[67] G. Kroemer, J.C. Reed, Mitochondrial control of cell death, Nat. Med. 6 (2000) 513–519.
[68] R.J. Youle, A.M. Van Der Bliek, Mitochondrial fission, fusion, and stress, Science 337 (2012) 1062–1065.
[69] Q.-P. Qin, T. Meng, M.-X. Tan, Y.-C. Liu, X.-J. Luo, B.-Q. Zou, H. Liang, Synthesis and *in vitro* biological evaluation of three 4′-(4-methoxyphenyl)-2,2′:6′,2″-terpyridine iridium(III) complexes as new telomerase inhibitors, Eur. J. Med. Chem. 143 (2018) 1387–1395.
[70] Q.-P. Qin, T. Meng, M.-X. Tan, Y.-C. Liu, X.-J. Luo, B.-Q. Zou, H. Liang, Synthesis, crystal structure and biological evaluation of a new dasatinib copper(II) complex as telomerase inhibitor, Eur. J. Med. Chem. 143 (2018) 1597–1603.
[71] S.S. Syeda, G. Sánchez, K.H. Hong, J.E. Hawkinson, G.I. Georg, G. Blanco, Design, synthesis, and *in vitro* and *in vivo* evaluation of ouabain analogues as potent and selective Na, K-ATPase α4 isoform inhibitors for male contraception, J. Med. Chem. 61 (2018) 1800–1820.
[72] T. Meng, Q.-P. Qin, Z.-L. Chen, H.-H. Zou, K. Wang, F.-P. Liang, Discovery of high

in vitro and *in vivo* antitumor activities of organometallic ruthenium(II)-arene complexes with 5,7-dihalogenated-2-methyl-8-quinolinol, Dalton Trans. 48 (2019) 5352–5360.
[73] M. Ott, V. Gogvadze, S. Orrenius, B. Zhivotovsky, Mitochondria, oxidative stress and cell death, Apoptosis 12 (2007) 913–922.
[74] Z. Zhu, Z. Wang, C. Zhang, Y. Wang, H. Zhang, Z. Gan, Z. Guo, X. Wang, Mitochondrion-targeted platinum complexes suppressing lung cancer through multiple pathways involving energy metabolism, Chem. Sci. 10 (2019) 3089–3095.
[75] X.-Q. Song, Z.-Y. Ma, Y.-G. Wu, M.-L. Dai, D.-B. Wang, J.-Y. Xu, Y.-Z. Liu, New NSAID-Pt(IV) prodrugs to suppress metastasis and invasion of tumor cells and enhance anti-tumor effect *in vitro* and *in vivo*, Eur. J. Med. Chem. 167 (2019) 377–387.
[76] J.-Q. Wang, P.-Y. Zhang, L.-N. Ji, H. Chao, A ruthenium(II) complex inhibits tumor growth *in vivo* with fewer side-effects compared with cisplatin, J. Inorg. Biochem. 146 (2015) 89–96.
[77] Q.-P. Qin, Z.-F. Wang, M.-X. Tan, X.-L. Huang, H.-H. Zou, B.-Q. Zou, B.-B. Shi, S.-H. Zhang, Complexes of lanthanides(III) with mixed 2, 2′-bipyridyl and 5, 7-dibromo-8-quinolinoline chelating ligands as a new class of promising anti-cancer agents, Metall 11 (2019) 1005–1015.
[78] F.-X. Wang, M.-H. Chen, Y.-N. Lin, H. Zhang, C.-P. Tan, L.-N. Ji, Z.-W. Mao, Dual functions of cyclometalated iridium(III) complexes: anti-metastasis and lysosome-damaged photodynamic therapy, ACS Appl. Mater. Interfaces 9 (2017) 42471–42481.
[79] M. Li, C. Du, N. Guo, Y. Teng, X. Meng, H. Sun, S. Li, P. Yu, H. Galons, Composition design and medical application of liposomes, Eur. J. Med. Chem. 164 (2019) 640–653.
[80] G. Compain, N. Oumata, J. Clarhaut, E. Péraudeau, B. Renoux, H. Galons, Sébastien Papot, A β-glucuronidase-responsive albumin-binding prodrug for potential selective kinase inhibitor-based cancer chemotherapy, Eur. J. Med. Chem. 158 (2018) 1–6.
[81] N. Oumata, K. Bettayeb, Y. Ferandin, L. Demange, A. Lopez-Giral, M.-L. Goddard, V. Myrianthopoulos, E. Mikros, M. Flajolet, P. Greengard, L. Meijer, H. Galons, Roscovitine-derived, dual-specificity inhibitors of cyclin-dependent kinases and casein kinases 1, J. Med. Chem. 51 (2008) 5229–5242.
[82] V. Spanò, M. Pennati, B. Parrino, A. Carbone, A. Montalbano, V. Cilibrasi, V. Zuco, A. Lopergolo, D. Cominetti, P. Diana, G. Cirrincione, P. Barraja, N. Zaffaroni, Preclinical activity of new [1,2]oxazolo[5,4-e]isoindole derivatives in diffuse malignant peritoneal mesothelioma, J. Med. Chem. 59 (2016) 157223–157238.
[83] V. Spanò, B. Parrino, A. Carbone, A. Montalbano, A. Salvador, P. Brun, D. Vedaldi, P. Diana, G. Cirrincione, P. Barraja, Pyrazolo[3,4-h]quinolines promising photosensitizing agents in the treatment of cancer, Eur. J. Med. Chem. 102 (2015) 334–351.
[84] B. Parrino, A. Attanzio, V. Spanò, S. Cascioferro, A. Montalbano, P. Barraja, L. Tesoriere, P. Diana, G. Cirrincione, A. Carbone, Synthesis, antitumor activity and CDK1 inhibiton of new thiazole nortopsentin analogues, Eur. J. Med. Chem. 138 (2017) 371–383.
[85] Q.-P. Qin, B.-Q. Zou, Z.-F. Wang, X.-L. Huang, Y. Zhang, M.-X. Tan, S.-L. Wang, H. Liang, High *in vitro* and *in vivo* antitumor activities of luminecent platinum(II) complexes with Jatrorrhizine derivatives, Eur. J. Med. Chem. 183 (2019) 111727. https://doi.org/10.1016/j.ejmech.2019.111727.
[86] Q.-P. Qin, Z.-F. Wang, X.-L. Huang, M.-X. Tan, Z.-H. Luo, S.-L. Wang, B.-Q. Zou, H. Liang, Two telomerase-targeting Pt(II) complexes of jatrorrhizine and berberine derivatives induce apoptosis in human bladder tumor cells, Dalton Trans. (2019). https://doi.org/10.1039/C9DT02381J.
[87] G.M. Sheldrick, SHELXTL-97, Program for Refinement of Crystal Structures, University of Göttingen, Germany, 1997.
[88] G.M. Sheldrick, SHELXS-97, Program for Solution of Crystal Structures, University of Göttingen, Germany, 1997.